24th INTERNATIONAL CONGRESS ON SOUND AND VIBRATION
23–27 July 2017, London

ON THE DISTINCTION OF AXISYMMETRIC WAVES WITHIN A FLUID-FILLED PIPE USING WAVENUMBER MEASUREMENT

M.Salimi *, J. M. Muggleton and E. Rustighi

University of Southampton, Institute of Sound and Vibration Research, , Highfield, Southampton, UK,
email: ms5c14@soton.ac.uk

Axisymmetric waves have characteristics, which are of practical interest when assessing the condition of a buried plastic water pipe. At low frequencies, well below the ring frequency, these waves are dominant. They are well couple to the fluid, pipe wall and surrounding medium and carry a high amount of energy when compared to other waves. Due to substantial differences in the wavenumber of the $s=1,2$ waves a new experimental method has been developed to distinguish between the pipe wall motion that arises from each axisymmetric wave. The results from experimental studies are compared with the theoretical predictions and a good agreement has been found. The outcomes of this investigation clarify the characteristics of the dominant axisymmetric wave within the buried pipes and thereby the waves generated within the surrounding medium. Moreover, decomposition of the two waves will help quantify the value of pressure within the fluid. Further application of this distinction is interpretation of the characteristics of the excitation source.

Keywords; axisymmetric waves decomposition; plastic water pipe.

1. Introduction

Intensive research has been carried out as part of the mapping the underworld project, aimed at identifying the location of buried utilities without the need for excavation [1]. One of the potential techniques is a vibro-acoustic approach, which includes collection of the ground surface vibration, resulting from propagation of the low frequency acoustic waves within a buried water plastic pipe. Looking at the both phase and magnitude of the transfer function between these recorded surface motions and acoustic wave generator within the pipe provides information about the location of the pipe [2]. For the pipe detection to be effective, the nature of the acoustic wave generation within the plastic pipes must be known, *a priori*. At low frequencies, four types of waves are responsible for most of the energy transfer [3], [4]. Out of four types of wave, three of them are axisymmetric (denoted by $n=0$, showed in Fig. 1-(b)). Out of these three, two waves termed $s=1,2$ usually carry high amounts of energy relative to the third $s=0$, a torsional wave. The wave termed $n=0$, $s=1$ is a fluid-borne wave with both axial and the radial motion [3], [4]. The axisymmetric wave termed $s=2$ is predominantly a shell compressional wave with small radial motion. Coupling between the fluid to the pipe wall can be achieved, as dictated by the Poisson's ratio and the Young's modulus of the pipe wall and also bulk modulus of the fluid. The axisymmetric torsional wave, termed $s=0$, is uncoupled to the fluid. Hence, the energy associated with this wave type is exclusively within the shell [3], [4]. The $n=1$ wave is a flexural wave, with the fluid inside exerting a mass loading effect. Waves with a circumferential mode greater than one ($n \geq 2$), cut on at higher frequencies. The speed and attenuation of these waves are associated with the real and imaginary components of the wavenumber respectively [5]. Due to the predominance of the axisymmetric waves within the buried plastic pipes at low frequencies, this research developed a candidate technique to decompose the contribution of $s=1,2$ waves on the pipe wall motion. The outcomes from this investigation provides better understanding of the detected waves at the ground surface, from vibration of a buried plastic water pipe. Prior to decomposing of the s=1,2 waves, a prototype models is required to express dynamic behaviour of a fluid filled pipes at low frequency.

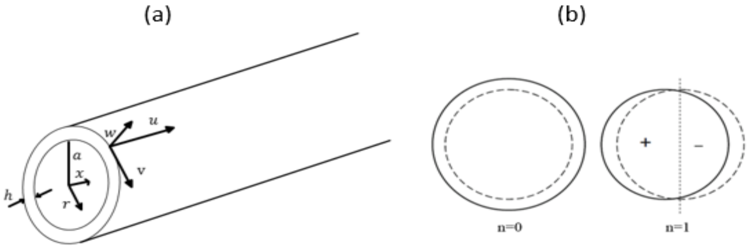

Figure 1 (a). Fluid-filled pipe coordinate system. (b) circumferential mode shapes of n = 0 and n=1. The modal shapes +/– illustrate the correspond phase of the motion in the relative region. —–, udeformed character; – –, deformed character.

2. Dynamic behaviour of fluid filled

The dynamic behaviour of a fluid filled pipe has been previously investigated in references [7-8]. In this paper, the models developed by Pinnington and Briscoe [6] are used for further analysis. In their model Kennard's equations are utilised, therefore the contribution from the bending wave, and the rotational inertia and shear transfer of the pipe are disregarded and only validated at well below the ring frequency. The equations provided here contain the parameters investigated in this paper, for further analysis. For a semi-infinite fluid filled pipe illustrated in Fig. 1-(a), the axial and radial displacement of the pipe wall and the axial displacement of the fluid arises from propagation of the $s=1,2$ wave in the positive x direction can be expressed by [6]:

$$u=\sum_{s=1}^{2}U_s e^{\mathrm{i}(\omega t-k_s x)},\ w=\sum_{s=1}^{2}W_s e^{\mathrm{i}(\omega t-k_s x)},u_f=\sum_{s=1}^{2}U_{sf} e^{\mathrm{i}(\omega t-k_s x)} \tag{1}$$

U_s and W_s are the amplitude of the pipe wall displacement, arise from $s=1,2$ waves in the axial and radial direction respectively. k_s is the wavenumber associated to the axisymmetric waves , expressed in Eq.(3). $U_{sf}=\dfrac{1}{\rho_f\omega^2}\dfrac{dp(x)}{dx}$; where ρ_f and ω are the fluid density and angular frequency respectively, $p(x)$ is the pressure within the fluid and is given by [6]:

$$p(x)=\sum_{s=1}^{2}P_f e^{\mathrm{i}(\omega t-k_s x)} \tag{2}$$

and $P_f=P_s J_0(k_s^r r)$; where P_s , J_0 and r are the amplitude of the fluid pressure arising from $s=1,2$ waves, a Bessel function of order zero and the radial distance in cylindrical coordinate system respectively. k_s^r is the radial wavenumber expressed via fluid wavenumber and the axisymmetric wavenumber by: $\left(k_s^r\right)^2=k_f^2-k_s^2$. k_s is the wavenumber associated to the fluid borne wave and the shell borne wave and is given by [6]:

$$k_1^2=k_f^2\left(\frac{1+\beta-v^2-\Omega^2}{1-v^2-\Omega^2}\right)\ \text{for}\ (s=1)\quad \text{and}\quad k_2^2=k_L^2\left(\frac{1-\Omega^2+\beta}{1+\beta-\Omega^2-v^2}\right)\ \text{for}\ (s=2) \tag{3}$$

where k_f and k_L are the fluid wavenumber and the compressional wavenumber in a flat plate respectively. v is the Poisson's ratio of the pipe wall, Ω is a normalized ring frequency; $\Omega = k_L a$, where a is the pipe mean radiuses. β called fluid loading which is given by [6]: $\beta = \frac{2B_f a}{Eh}(1-v^2)$; where B_f, E and h are the fluid bulk modulus; pipe wall Young's modulus and its thickness respectively. The relationship between fluid pressure and radial motion of the pipe wall associated with the s=1,2 waves can be represented as [6]:

$$\frac{W_1}{W_2} = -\frac{P_1}{P_2}\left[\frac{\beta}{1-v^2-\Omega^2}\right] \tag{4}$$

where P_1 and P_2 are the fluid pressure associated to the s=1,2 waves. The axial and radial motion of the pipe wall arising from the s=1,2 wave are related together by [6]:

$$\frac{U_1}{U_2} = \frac{W_1}{W_2}\frac{k_2}{k_1}\frac{v^2}{(1+\beta-\Omega^2)} \tag{5}$$

At low frequency when $\Omega << 1$ and by assuming $v^2 < \beta$, the relative energy associated to each wave can be expressed by [6]: $\frac{e_1}{e_2} = \left(\frac{W_1}{W_2}\right)^2 \frac{v^2(1-v^2)^2}{\beta(1+\beta)^2}$.

2.1 Axial excitation of the pipe wall

Applying axial excitation to the pipe wall, gives zero pressure within the fluid at $x=0$. Applying this boundary condition to Eq.(2) provides $P_1 = -P_2$ at x=0 and therefore Eq.(4) decreases to [6]: $\left[\frac{W_1}{W_2}\right]_p = \left[\frac{\beta}{1-v^2-\Omega^2}\right]$, where the subscript p illustrates pipe wall excitation. Substituting Eq.(4) into Eq.(5) gives the relative amplitudes of the each wave in axial direction as [6]: $\left[\frac{U_1}{U_2}\right]_p = \left(\frac{v^2}{1+\beta-\Omega^2}\right) \cdot \left(\frac{\beta}{1-v^2-\Omega^2}\right)\frac{k_2}{k_1}$.

2.2 Fluid excitation

The axial stress within the pipe wall at any position along the pipe is given by [6]:

$$\sigma(x) = -\mathrm{i}\rho_\mathrm{m}\omega^2\left[\frac{U_1 e^{-\mathrm{i}k_1 x}}{k_1} + \frac{U_2 e^{-\mathrm{i}k_2 x}}{k_2}\right] \tag{6}$$

Exciting of the contained fluid gives zero axial stress, in the shell wall, at the point of excitation. Therefore, by setting $\sigma(0) = 0$ in Eq. (6), release [6]: $\left[\frac{U_1}{U_2}\right]_f = -\frac{k_1}{k_2}$, where the subscript f illustrates fluid excitation. The relative wave amplitudes in the radial direction is established via substituting Eq. (6) into Eq. (5), as [6]: $\left[\frac{W_1}{W_2}\right]_f = \left(\frac{k_2}{k_1}\right)^2 \frac{(1+\beta-\Omega^2)}{v^2}$.

3. Model parameters

The material properties of the used MDPE pipe and the contained fluid are tabulated in Table 1.

Table 1 Material properties of MDPE pipe.

Parameter	Description of parameter	MDPE	Water	Air
a	Mean radius (m)	8.45×10^{-2}	-	-
h	Wall thickness (m)	1.1×10^{-2}	-	-
E	Young's modulus (Gpa)	1.6	-	-
η	Material loss factor	0.06	-	-
v	Poisson's ratio	0.4	-	-
B	Bulk modulus	-	2.18×10^{9}	1.42×10^{5}
ρ	Density (m^3)	880	1000	1.29

The ratios derived in Sections 2.1 and 2.2 are calculated in accordance with the data provided in Table 1, and listed in Table 2

Table 2 Ratios of variables related to the axisymmetric fluid and shell borne wave within the MDPE pipe loaded via different excitation sources at frequency of (a) 10 Hz and (b) 400 Hz.

	$\left\|\frac{W_1}{W_2}\right\|$	$\left\|\frac{U_1}{U_2}\right\|$	$\left\|\frac{P_1}{P_2}\right\|$	$\left\|\frac{e_1}{e_2}\right\|$
Structural excitation (a) of the water filled pipe (b)	20.9 21.4	0.03 0.03	1 1	008 008
Fluid excitation of (a) the water filled pipe (b)	2531 2590	4.66 4.71	120 120	116 121

The data presented in Table 2 illustrates the fact that the axial displacement of the wall of water-filled pipe, induced via structural vibration, is predominantly due to the $s=2$ wave. Furthermore, the radial displacement of the pipe wall is primarily due to the $s=1$ wave, even though it only carries a small amount of energy.

When the pipe loaded with the fluid excitation, the $s=1$ wave becomes predominant in both axial and circumferential direction and most of the energy store in the fluid. However, the contribution from the $s=2$ wave on the axial displacement of the pipe wall is not negligible.

In the next part, a technique is presented to discriminate between the $s=1,2$ waves using experimental data. As a first try, selecting an ideal situation where both wave types have the same magnitude might help achieve successful wave decomposition; however, none of the ratios presented in Table, 2-3 are equal or close to unity. Thus, the best option for post processing, is analysing the data obtained from axial displacement of the pipe wall when the excitation is applied to the fluid.

4. Axisymmetric wave decomposition

The experimental arrangement consists of a 2.12 m water filled MDPE pipe. Geometrical and material properties of the pipe are illustrated in Table 1. The test specimen was assembled by placing four B&K accelerometers axially around the circumference of the pipe wall. Spatial averaging of the data from these four accelerometers allows us to reduce the effects from higher order modes on the pipe wall displacement. This measurement was taken at four locations along the pipe, with interval distances of $\Delta x = 0.3m$ between each adjacent measurement point, depicted in Fig. 2. The optimal distance for transducer placement is given by [8]: $0.1\pi < k.\Delta x < 0.8\pi$; where k is the medium wave-number and Δx is the distance between adjacent transducers.

Measurement of the flexural wave in a beam and a plate within the near field region was performed by Pavic [9]. The results illustrate that the effect of the near field wave cannot be discarded unless the location of the measurement point is at a distance equal to half a wavelength from any discontinuity. Therefore, measurements were taken at 40 cm distance from each end of the pipe. The effects from evanescent waves might become significant for either short pipes or at lower frequencies.

In this experiment, the cylinder was subjected to the fluid excitation at one end, via an underwater loudspeaker followed by recording the axial acceleration of the pipe wall as illustrated in Fig. 2. The time extended signal used to internally excite the pipe composed of a linear sweep sine, ranging from 10 Hz to 400 Hz, each lasting two seconds. The signal then was recorded using a sampling rate of 1 kHz and a low pass filter was imposed at 400 Hz to prevent aliasing.

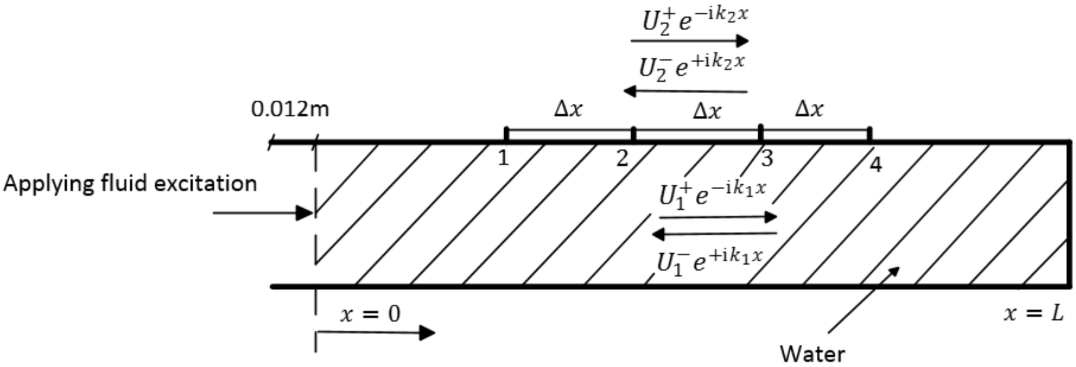

Figure 2 Experimental arrangement used for monitoring the axial motion of the shell comprises the s=1,2 waves.

The recorded axial acceleration of the pipe wall composes of four independent elements, namely: two axisymmetric waves in the axial direction, travelling up and down along the pipe. Since the accelerometer measures the acceleration of the pipe wall, to obtain the pipe wall displacement, the data outputted from the transducers is divided by ω^2 . However, as we are interested in the amplitude ratio of these two axisymmetric wave, this division is not necessary and has been performed for the sake of clarity. The general form for decomposition of the amplitude of the each axisymmetric wave can be achieved by: 1- substitution of the transfer functions $Q(x_1),\ldots,Q(x_4)$, which are obtained via measurement of the axial acceleration of the pipe wall, at locations $x_1,\ldots,x_4$, with respected to the applied voltage to the loud speaker followed by dividing them by ω^2 , in the matrix in Eq. (7). 2- Substitution of the wavenumbers of the two axisymmetric waves, k_1 and k_2 from the analytical simulation given in Eq. (3), into Eq. (7). Therefore, the only unknown terms are U_1 and U_2 which represent the amplitudes of the axisymmetric waves with respect to the applied voltage and the superscripts $+$ and $-$ represent the waves travelling in the positive and negative direction.

$$\frac{1}{-\omega^2}\begin{bmatrix} Q(x_1) \\ \vdots \\ Q(x_4) \end{bmatrix} = \begin{bmatrix} e^{-ik_1x_1} & e^{ik_1x_1} & e^{-ik_2x_1} & e^{ik_2x_1} \\ \vdots & \vdots & \vdots & \vdots \\ e^{-ik_1x_4} & e^{ik_1x_4} & e^{-ik_2x_4} & e^{ik_2x_4} \end{bmatrix} \begin{bmatrix} U_1^+ \\ U_1^- \\ U_2^+ \\ U_2^- \end{bmatrix} \tag{7}$$

By performing matrix inversion into Eq. (7), the amplitude of each axisymmetric wave can be expressed by:

$$\begin{bmatrix} U_1^+ \\ U_1^- \\ U_2^+ \\ U_2^- \end{bmatrix} = \frac{1}{-\omega^2}\begin{bmatrix} e^{-ik_1x_1} & e^{ik_1x_1} & e^{-ik_2x_1} & e^{ik_2x_1} \\ \vdots & \vdots & \vdots & \vdots \\ e^{-ik_1x_4} & e^{ik_1x_4} & e^{-ik_2x_4} & e^{ik_2x_4} \end{bmatrix}^{-1} \begin{bmatrix} Q(x_1) \\ \vdots \\ Q(x_4) \end{bmatrix} \tag{8}$$

The ratio of the U_1^+/U_2^+ and U_1^-/U_2^- obtained from Eq. (8) is plotted in Figure 3 using the blue and red dotted lines respectively. Discrepancy between the data from experimental study and theory is observed at frequencies above 120 Hz. The observed peaks at 120 Hz, 380 Hz are related to the cut on frequency of the $n=2,3$ modes. The cut on frequency of the higher order modes for the empty and the water filled MDPE pipe when it is surrounded by air are provided in Section 4.1. Furthermore, the peaks observed at intervals of 63 Hz corresponded to the resonance frequency of the fluid column, which occurs at the integral numbers of half wavelengths within the fluid.

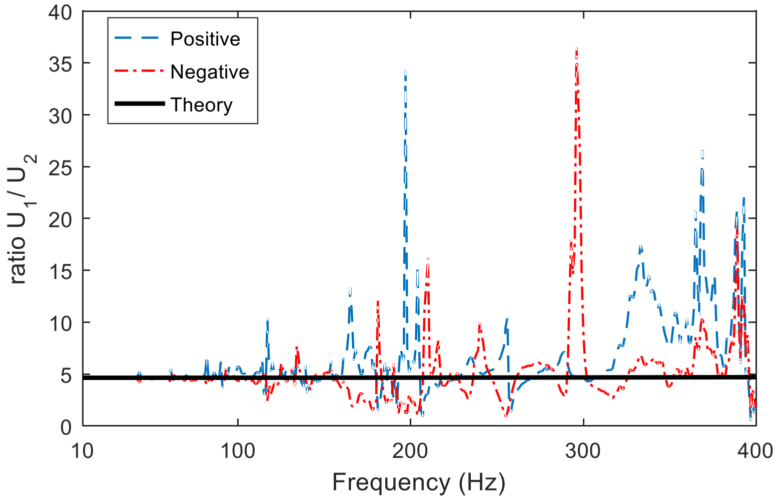

Figure 3 The ratio between s=1,2 waves contributes to the axial displacement of the pipe wall, for fluid excitation at frequency 10 Hz to 400Hz

4.1 Cut on frequency of flexural modes of thin walled shell

As illustrated in Figure 3, the measured data was slightly deviated from the theory. Therefore, an investigation was carried out to find the cut on frequency of the higher order modes within the plastic pipe when it is empty and when it is filled with water, which is given by [10]:

$$f_c = f_{ring}\sqrt{\frac{\psi_s^2 n^2 (n^2-1)^2}{1+n^2+\mu n+\psi_s^2 (n^2-1)^2}} \tag{9}$$

where $\mu = \frac{a\rho_f}{h\rho_s}$ is the fluid –shell mass ratio, where ρ_f and ρ_s are the density of the fluid and the pipe wall respectively. $f_{ring} = \frac{c_L}{2\pi a}$ is the pipe ring frequency, where $c_L = \sqrt{E/\rho_s}$, and $\psi_s^2 = \frac{h^2}{12a^2}$ is the shell thickness parameter. Similar formula is established by Moser [11] (eq.4 of the mentioned paper). Substituting the parameter, using Table 1, the cut on frequency of the higher modes for the empty and the water filled pipe is:

Table 3 Cut on frequency of the MDPE pipe when it is empty and when filled with the water.

Mode number	n=2	n=3	n=4	n=5
Cut on frequency of the empty pipe (Hz)	255	720	1374	2209
Cut on frequency of the water filled pipe (Hz)	120	380	792	1364

5. Conclusion

Due to well coupling of the $s=1,2$ waves, applying any type of excitation to the water-filled pipe will generate these two wave. In this study, attempts are made to distinguish between the contributions from the two waves on the vibration of the pipe wall. The results from experimental study are compared with theoretical predictions and a good agreement has been obtained. Extension of this practical measurement, for decomposition of the effect of the $s=1,2$ waves on the axial and radial motion of the pipe wall, via other source sensor sets, is under investigation.

The data from this examination highlight the dominant axisymmetric waves within the pipe wall and clarifies the type of generated conical wave within the surrounding medium. Further applications of this decomposition are elaboration of the source of excitation within the pipe and quantification the induced pressure within the pipe.

REFERENCES

1 C. D. F. Rogers et al., “Condition assessment of the surface and buried infrastructure - A proposal for integration,” Tunn. Undergr. Sp. Technol., vol. 28, no. 1, pp. 202–211, 2012.

2 J. M. Muggleton, M. J. Brennan, and Y. Gao, “Vibration radiation from buried plastic water pipes: an experimental investigation at the ground surface,” Proc. Int. Conf. Noise Vib. Eng. ISMA 2012, pp. 1223–1237, 2012.

3 C. R. Fuller, F. J. J. Fahy, C. R. FULLER, and F. J. J. Fahy, “Characteristics of wave propagation and energy distributions in cylindrical elastic shells filled with fluid,” J. ofSound Vib., vol. 81, no. 4, pp. 501–518, 1982.

4 C. R. FULLER, “The input mobility of an infinite cylindrical shell filled with fluid,” J. Sound Vib., vol. 87, pp. 409–427, 1983.

5 J. M. Muggleton, M. J. Brennan, and P. W. Linford, “Axisymmetric wave propagation in fluid-filled pipes: Wavenumber measurements in in vacuo and buried pipes,” J. Sound Vib., vol. 270, no. 1–2, pp. 171–190, 2004.

6 R. J. Pinnington and A. R. Briscoe, “Externally Applied Sensor for Axisymmetric Waves in a Fluid Filled Pipe,” J. Sound Vib., vol. 173, no. 4, pp. 503–516, 1994.

7 T. C. Lin and G. W. Morgan, “Wave Propagation through Fluid Contained in a Cylindrical, Elastic Shell,” J. Acoust. Soc. Am., vol. 28, no. 6, p. 1165, 1956.

8 H. BODEN, “Characterization of fluid machines as sources of fluid borne noise,” report TRITA-TAK-8906, Royal Institute of Technology, Stockholm, 1989.

9 G. Pavić, “Measurement of structure borne wave intensity, Part I: Formulation of the methods,” J. Sound Vib., vol. 49, no. 2, pp. 221–230.

10 G. Pavić, “Vibroacoustical energy flow through straight pipes,” J. Sound Vib., vol. 154, no. 3, pp. 411–429, 1992.

11 V. M. Moser and M. H. K. Ginters, “Zur Schallausbreitung in flussigkeitsgefullten kreiszylindrischen Rohren.”